The FASEB Journal

FASEB
Federation of American Societies for Experimental Biology

RESEARCH ARTICLE OPEN ACCESS

From Single-Cell Clusters to Causality: ITCH Engagement for CKD Uncovered by Integrative Analysis of MR and MAGMA

Xia Zhang | Dongdong Zhang | Jiazhen Shang | Zhitao Zeng | Shouyu Chai | Xincong Lv | Zhimei Lv | Rong Wang

Department of Nephrology, Shandong Provincial Hospital Affiliated to Shandong First Medical University, Jinan, Shandong, China

Correspondence: Zhimei Lv (lyuzhimei@126.com) | Rong Wang (wangrong_sd@126.com)

Received: 8 July 2025 | **Revised:** 21 December 2025 | **Accepted:** 7 January 2026

Keywords: chronic kidney disease | fibrosis | ITCH | MAGMA | mendelian randomization | Pseudobulk | scRNA-seq | tubular injury

ABSTRACT

Chronic kidney disease (CKD) is a leading and rapidly rising contributor to global mortality, yet actionable molecular targets remain limited. Here, we integrated human kidney single-cell RNA sequencing (scRNA-seq) with genetic association and causal inference frameworks to prioritize putative CKD susceptibility genes. To mitigate cell-level pseudoreplication inherent to small-donor scRNA-seq datasets, we primarily implemented a donor-aware pseudobulk strategy to identify differentially expressed genes (DEGs) between CKD and control kidneys, and subsequently prioritized candidates by convergent evidence from Mendelian randomization (MR) and MAGMA gene-level association analyses using CKD-related GWAS summary statistics. Across these complementary layers, ITCH emerged as a high-confidence candidate, showing consistent support from transcriptomic dysregulation and genetic evidence. We further performed immunohistochemistry-based validation in an experimental kidney injury model, providing additional support for ITCH upregulation in diseased kidneys. Finally, to explore potential pharmacological modulation in a hypothesis-generating manner, we conducted DSigDB-based drug enrichment followed by molecular docking and 50-ns molecular dynamics simulations to evaluate structural compatibility and complex stability, nominating hesperetin as a higher-priority compound for subsequent experimental testing. Collectively, our multi-omics integration supports ITCH as a plausible gene involved in CKD pathobiology and provides a rationale for the hypothesis that targeting ITCH could alter disease progression, which warrants future experimental investigation.

1 | Introduction

Chronic kidney disease (CKD) is a global health burden affecting approximately 10% of the population and is associated with increased morbidity, mortality, and healthcare costs [1]. The number of deaths expected to result from a CKD diagnosis by 2040, which is projected to increase to 2.2 million in the best-case scenario and 4 million in the worst-case scenario. CKD will become the fifth leading cause of years of life lost globally in 2040 [2]. Progression of CKD toward end-stage kidney disease (ESKD) is characterized by structural and functional deterioration of renal tissue, including tubular atrophy, glomerulosclerosis, vascular rarefaction, and interstitial fibrosis. CKD can be the consequence of a single etiology, but it frequently relates rather to sequential injuries accumulating over the life course or to the presence of concomitant risk factors [3], including hypertension, diabetes, injury and complex genetic factors [4–6]. Despite decades of research, the molecular mechanisms driving these

Abbreviations: MAGMA, Multi-marker Analysis of Genomic Annotation; PCA, Principal Component Analysis; UMAP, Uniform Manifold Approximation and Projection.

Xia Zhang and Dongdong Zhang first authors.

pathological processes remain incompletely understood, limiting the development of targeted interventions that can halt or reverse disease progression. Due to the large number of affected patients and the investment in treatment, it is of medical and economic interest to endeavor to achieve effective slowing down of the course of CKD or even reversal of renal failure by unremitting excavation.

Genome-wide association studies (GWAS) have identified numerous susceptibility loci associated with kidney function and CKD risk [7]. However, most GWAS signals lie in non-coding regions, complicating the identification of effector genes and pathways. Moreover, GWAS alone does not resolve the cellular origin or causal direction of gene–trait associations. Advances in single-cell RNA sequencing (scRNA-seq) have enabled high-resolution profiling of cell-type–specific gene expression patterns in human kidneys, offering a unique opportunity to localize disease-relevant molecular signals [8]. Meanwhile, causal inference methods such as Mendelian randomization (MR) provide a framework for assessing whether genetically regulated gene expression contributes to disease risk [9]. Integrating these approaches with gene-level enrichment tools such as MAGMA offers a powerful strategy to bridge statistical associations with functional biology [10].

In this study, we integrated CKD versus control kidney scRNA-seq with CKD-related GWAS summary statistics to identify transcriptomic alterations and prioritize candidate susceptibility genes. We employed a donor-aware pseudobulk strategy as the primary differential expression framework to mitigate cell-level pseudoreplication and combined these results with MR and MAGMA to obtain convergent genetic and transcriptomic support. Using this multi-layer framework, we identified ITCH as a high-confidence candidate gene implicated in CKD pathobiology. Finally, to generate pharmacological hypotheses, we performed DSigDB-based drug enrichment and conducted molecular docking and 50-ns molecular dynamics simulations to evaluate structural compatibility and complex stability for selected compounds, thereby nominating candidates for subsequent experimental validation in CKD-relevant models.

2 | Methods and Materials

2.1 | Sample Collection and scRNA-Seq

Publicly available human kidney scRNA-seq data (GSE199711) [11] were obtained from GEO, including five donors (CKD: $n = 3$, GSM5982486/87/88; HC: $n = 2$, GSM5982489/90) derived from cortex/medulla tissues and analyzed in R using Seurat (v4.3.0). After quality control, 15 896 cells were retained, comprising 9926 CKD cells (GSM5982486: 1889; GSM5982487: 3935; GSM5982488: 4102) and 5970 HC cells (GSM5982489: 3348; GSM5982490: 2622). Raw 10× matrices were loaded into Seurat with an initial filter of > 300 detected genes (min. features = 300). Mitochondrial and hemoglobin fractions were calculated using PercentageFeatureSet, and cells were filtered using nFeature_RNA > 300, nCount_RNA < 30 000, percent.mt < 20%, and percent.HB < 3%. Data were normalized with SCTransform (glmGamPoi) regressing out percent.mt, followed by PCA (npcs = 50), UMAP and Louvain clustering using the top 30 PCs (dims = 1:30; resolution = 0.8), and cell-type annotation based on canonical markers.

2.2 | Differential Expression Analyses

To provide an exploratory single-cell view, differential expression between CKD and HC was first assessed within each annotated cell type using Seurat FindMarkers (Wilcoxon rank-sum test; logfc.threshold = 0, min.pct = 0.1) with Benjamini–Hochberg adjustment, and genes were summarized using $|\log2FC| > 0.5$ and FDR < 0.05. To mitigate donor-level dependence and pseudoreplication, inferential DE was primarily conducted using a donor-aware pseudobulk strategy: raw counts were aggregated per donor within each cell type (Seurat AggregateExpression), such that each donor contributed one pseudobulk profile, followed by edgeR quasi-likelihood GLM testing (DGEList → filterByExpr → TMM normalization → estimateDisp → glmQLFit → glmQLFTest) using the same thresholds ($|\log2FC| > 0.5$ and FDR < 0.05). Concordance between single-cell and pseudobulk results was evaluated by comparing matched gene-wise log2FC estimates across cell types using faceted scatter plots.

2.3 | Mendelian Randomization Analysis of eQTL–CKD and eGFR Links

To prioritize genes with putative causal effects on CKD risk, two-sample MR [12] was performed using cis-eQTL instruments from eQTLGen (OpenGWAS), with CKD GWAS summary statistics (IEU OpenGWAS: ebi-a-GCST003374) and for serum creatinine-based estimated glomerular filtration rate (eGFR) (IEU Open GWAS ID: ebi-a-GCST003372) as outcomes [13] Instruments were selected per gene using a significance threshold $p < 1 \times 10^{-5}$ and LD clumping ($r^2 = 0.1$, window = 10 000 kb). Exposure and outcome datasets were harmonized (strand/allele alignment, ambiguous variants removed). The primary causal estimate was obtained by IVW when ≥ 2 SNPs were available; Wald ratio was used for single-SNP instruments. Sensitivity analyses included MR-Egger, weighted median, and weighted mode when applicable, along with Cochran's Q test for heterogeneity, Egger intercept for directional pleiotropy, and MR-PRESSO global test to detect horizontal pleiotropy/outliers.

2.4 | Gene Network Construction

To visualize functional relatedness among MR-prioritized genes, a gene–gene interaction network was generated (GeneMANIA, https://genemania.org/), and interactions were displayed as an integrated network to highlight potential shared biological modules.

2.5 | MAGMA Gene-Level and Gene-Set Enrichment Analysis

MAGMA (v1.10) was used to perform gene-level association analysis based on CKD GWAS summary statistics [10].

Gene-level Z-scores were calculated and subsequently tested for enrichment across 17 015 curated gene sets from MSigDB (v2023.1. Hs). Covariates including gene size, gene density (number of SNPs per gene), and minor allele frequency were included in the model. Gene sets with Bonferroni-adjusted p values less than 0.05 were considered markedly enriched. Results were visualized by Manhattan plots. MR- and MAGMA-derived candidates were intersected to obtain convergent priority genes.

2.6 | Colocalization Analysis

To investigate whether the genetic associations between ITCH expression and kidney traits (CKD and eGFR) share the same causal variants while minimizing confounding from linkage disequilibrium (LD), we applied a Bayesian colocalization approach [14]. Colocalization analyses were conducted within a predefined cis-region (±500 kb of the ITCH gene) using summary statistics from eQTL (eQTLGen Consortium) and GWAS datasets for CKD and eGFR. Variants with a minor allele frequency (MAF) < 0.05 were excluded. The posterior probability for colocalization (PP.H4) was estimated using the coloc R package (v5.1.0) [15], with PP.H4 > 80% considered strong evidence for colocalization. All analyses were performed in R (v4.3.0).

2.7 | Drug Enrichment, Molecular Docking, and Molecular Dynamics Simulations

Candidate compounds potentially modulating ITCH were prioritized by DSigDB-based drug–gene enrichment analysis [16]. The experimentally determined human ITCH structure (PDB ID: pdb_00003tug), corresponding to the catalytic HECT domain (approximately residues 523-903), was used for docking and simulations; BLASTP alignment against RefSeq NP_001244066.1 showed 99.21% sequence identity with 96% query coverage (378/381 identities, 0 gaps), supporting structural suitability. Five small molecules (pipemidic acid, pyrvinium, spiperone, torcetrapib, and hesperetin) were docked using CB-Dock2 (AutoDock Vina scoring) [17, 18], and top-ranked poses were retained with docking scores/pocket volumes recorded and interactions visualized in Discovery Studio. For leading candidates, all-atom MD simulations were performed in GROMACS v2020.6 using the AMBER99SB-ILDN force field, followed by 50-ns production runs for each ITCH–ligand complex. Trajectories were evaluated by backbone RMSD, protein–ligand hydrogen-bond counts, free-energy landscape (FEL) projection, and SASA.

2.8 | Immunohistochemical Staining

Paraffin-embedded kidney sections were deparaffinized, subjected to high-temperature antigen retrieval, and incubated overnight at 4° with primary antibody against ITCH (Proteintech, 20920-1-AP; 1:200). The next day, sections were sequentially incubated with a horseradish peroxidase (HRP)-conjugated secondary antibody, developed with 3,3′-diaminobenzidine (DAB) chromogen under microscopic monitoring, and counterstained with hematoxylin to visualize nuclei. After dehydration and mounting, antigen localization was assessed by light microscopy.

3 | Results

3.1 | Integrated Single-Cell and Genetic Causal Inference Prioritize CKD-Associated Cell-Type Programs and Candidate Genes

After quality control and unsupervised clustering, the scRNA-seq atlas resolved 12 major renal and immune cell populations, encompassing tubular epithelial subsets (proximal tubule, distal convoluted tubule (DCTs), thick ascending limb, principal and intercalated cells), glomerular podocytes, stromal/vascular compartments (fibroblasts, endothelial and vascular smooth muscle cells), and immune subsets (M2 macrophages, T cells, and B cells; Figure 1A). Donor-level compositional profiling revealed CKD-associated remodeling with a relative reduction of tubular epithelial compartments accompanied by an expansion of stromal and immune fractions across CKD donors (Figure 1B). To ensure robustness while accounting for donor-level dependence, we compared cell-level differential expression with a cell type–specific pseudobulk edgeR framework, observing consistent directionality of log2FC estimates between approaches and strong within-cell-type concordance (Figure 1C), which enabled reliable delineation of CKD transcriptional programs across nephron segments and immune/stromal populations (Figure 1D, Table S1). Integrating these donor-aware DEGs with eQTLGen-derived cis-instruments, two-sample MR incorporating pleiotropy-robust sensitivity analyses prioritized 12 genes passing primary IVW filtering (Figure 1E, Table S2), and network modeling further indicated that these candidates constitute a connected module with additional functional neighbors, supporting convergent genetic mechanisms implicated in CKD pathogenesis (Figure 1F).

3.2 | Multi-Omics Analysis Nominates ITCH as a Putative Causal CKD Gene

MAGMA gene-level analysis identified multiple CKD-associated genes (Figure 2A), and integration with MR-prioritized candidates converged on a single high-confidence gene, ITCH (Figure 2B). Concordantly, ITCH was upregulated in distal convoluted tubule (DCT) cell, intercalated cell, and M2 macrophage compared to HC, while downregulated in proximal tubular cell (Figure 2C). DCT constitutes the nephron segment that lies immediately downstream of the macula densa, holding the key to precise regulation of electrolyte balance and acid-alkali balance [19]. Bayesian colocalization supported a shared causal signal between the ITCH cis-eQTL and CKD/eGFR association at this locus (PP.H4 = 0.919 for CKD and 0.809 for eGFR; Figure 2D,E), reducing the likelihood of LD-driven confounding. Consistent with these findings, IVW-based MR showed that genetically predicted higher ITCH expression increased CKD risk ($\beta = 0.1763$, SE = 0.0619, $p = 0.0044$) and decreased eGFR ($\beta = -0.0148$, SE = 0.00349, $p = 1.81 \times 10^{-7}$; Table 1), collectively implicating ITCH as a deleterious determinant of kidney function.

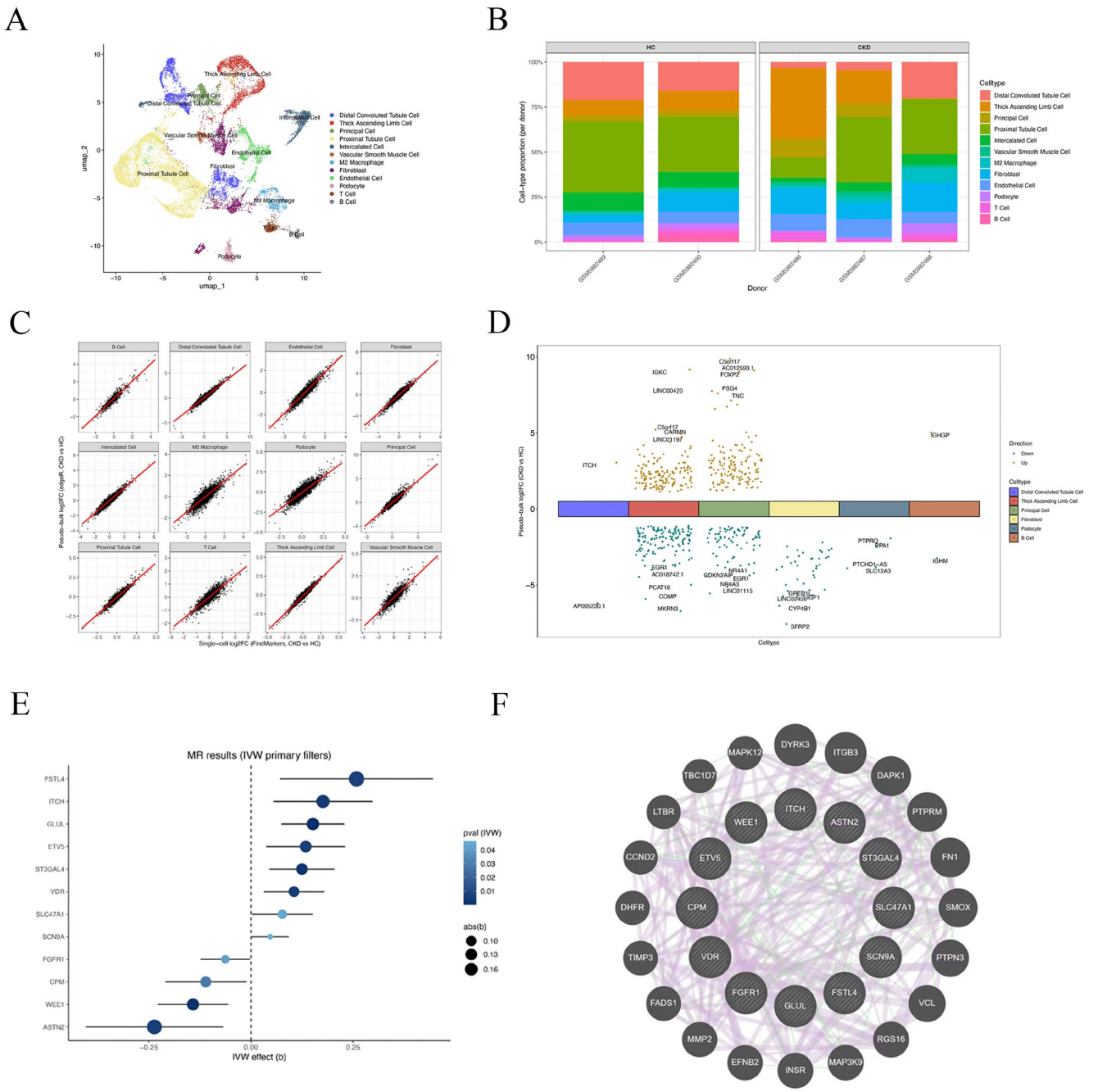

FIGURE 1 | Integrated single-cell and genetic analyses prioritize putative causal genes in CKD. (A) UMAP of 12 annotated kidney cell types from HC ($n = 2$) and CKD ($n = 3$). (B) Donor-level cell-type proportions in HC and CKD. (C) Agreement between cell-level and pseudobulk log2FC estimates across cell types (red line, $y = x$). (D) Pseudobulk CKD–HC differential expression across cell types, showing representative up- and down-regulated genes. (E) Two-sample MR (IVW) results using eQTL instruments; bubble size denotes the absolute IVW effect estimate ($|\beta|$) and color denotes the IVW p value. (F) GeneMANIA network of MR-prioritized genes showing functional connectivity.

3.3 | Drug Enrichment, Docking, and MD Prioritize Hesperetin as a Stable ITCH Binder

To explore potential pharmacological modulation of ITCH in CKD, we first performed DSigDB-based drug–gene enrichment analysis, which highlighted several compounds predicted to target ITCH (Figure 3A). We next conducted molecular docking to assess structural compatibility within putative ITCH binding pockets, yielding favorable binding poses for five selected compounds with AutoDock Vina scores ranging from −8.8 to −7.1 kcal/mol (Figure 3B–F), with pyrvinium and hesperetin showing the most negative docking scores. To further interrogate binding stability beyond static docking, we performed 50-ns MD simulations (Figure 4A–E) and evaluated backbone RMSD, protein–ligand hydrogen-bonding, Gibbs free-energy landscapes, and SASA. The ITCH–hesperetin complex showed a low and rapidly plateauing RMSD, sustained hydrogen-bond contacts, and convergence to a predominant low-energy basin with relatively stable SASA, consistent with a comparatively stable bound state (Figure 4B). In contrast, ITCH–pyrvinium exhibited

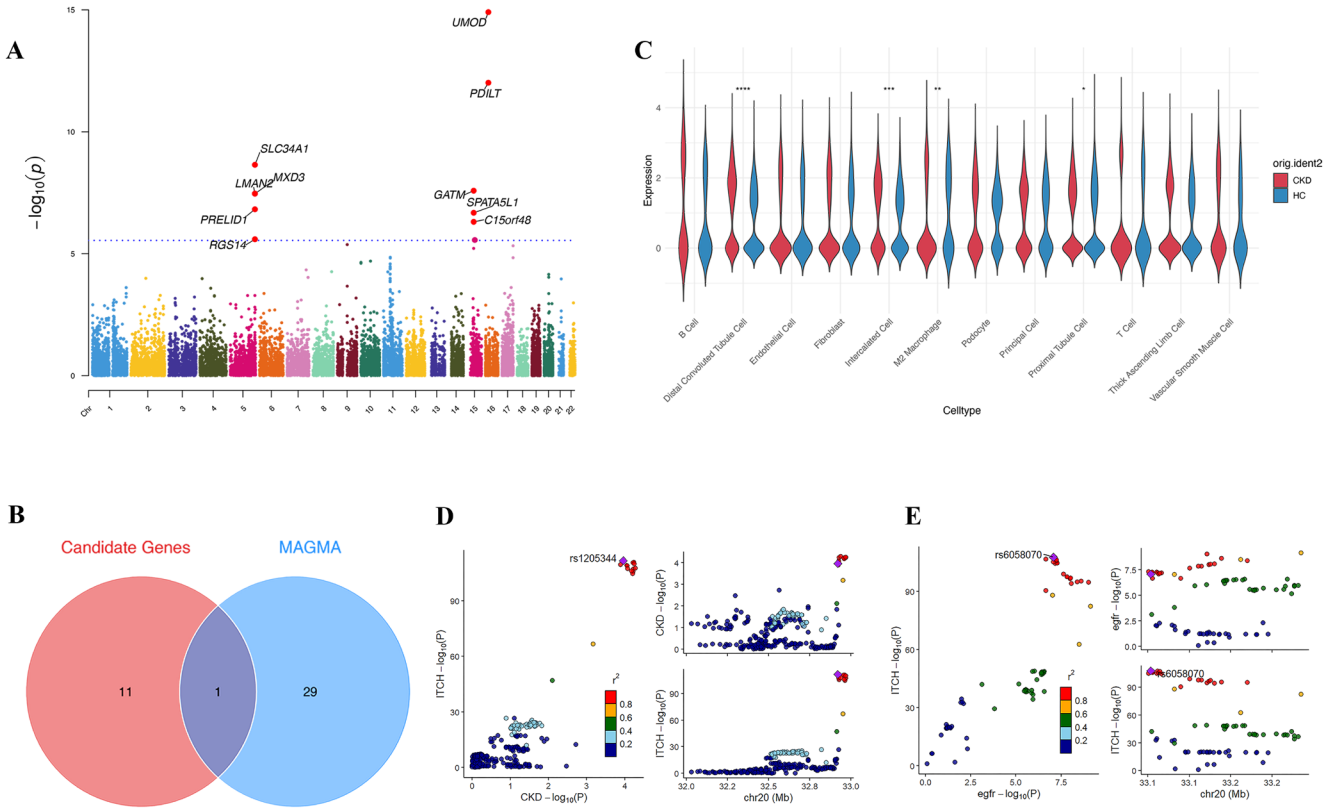

FIGURE 2 | Multi-omics prioritization and colocalization nominate ITCH as a CKD risk gene. (A) MAGMA gene-level Manhattan plot for CKD. (B) Overlap of MR-prioritized and MAGMA-significant genes, identifying ITCH as the sole convergent gene. (C) Cell type–resolved ITCH expression in HC vs. CKD (violin plots). (D) Regional association and colocalization at the ITCH locus for CKD. (E) Regional association and colocalization at the ITCH locus for eGFR.

TABLE 1 | Table MR results of ITCH with CKD and eGFR.

Exposure	Outcome	Method	*b*	SE	*p*
ITCH	eGFR	IVW	−0.0148440993978908	0.003486592	1.81E-07
ITCH	CKD	IVW	0.176321666	0.061937312	4.4E-03

pronounced RMSD fluctuations with sparse hydrogen-bonding and a more heterogeneous free-energy landscape accompanied by SASA perturbations (Figure 4A). ITCH–spiperone showed evident late-stage RMSD deviations and SASA changes, suggesting increased conformational variability during the trajectory (Figure 4E). On balance, these in silico analyses prioritize hesperetin as a comparatively stable candidate ITCH binder, warranting subsequent experimental validation in CKD-relevant models.

3.4 | Experimental Validation of ITCH in CKD

Based on our preceding findings, we performed IHC on mouse kidney tissues. The results showed the expression of ITCH was significantly upregulated in the kidneys of CKD mice (induced by Unilateral Ureteral Obstruction) compared with the controls (Figure 5A–C). This serves as an experimental validation of our bioinformatic findings described above.

4 | Discussion

In this study, we employed an integrative, multi-omic framework combining scRNA-seq, MAGMA analysis, and Mendelian randomization to elucidate the genetic and molecular underpinnings of CKD. This approach enabled high-resolution dissection of cell-type–specific transcriptomic alterations and identification of causally associated genes. Among the genes uncovered, ITCH emerged as a critical candidate—uniquely supported by both genetic association and transcriptomic causality—positioning it as a robust susceptibility gene in CKD pathogenesis. Its pronounced expression in DCTs—an understudied compartment in CKD—highlights its latent relevance.

ITCH (Itchy E3 ubiquitin protein ligase), also designated as Atrophin-1-interacting protein 4 (AIP4), belongs to the Nedd4 family of HECT-domain E3 ubiquitin ligases [20]. Structurally, ITCH comprises an N-terminal lipid-binding C2 domain, a proline-rich region, two WW motifs, and a C-terminal HECT

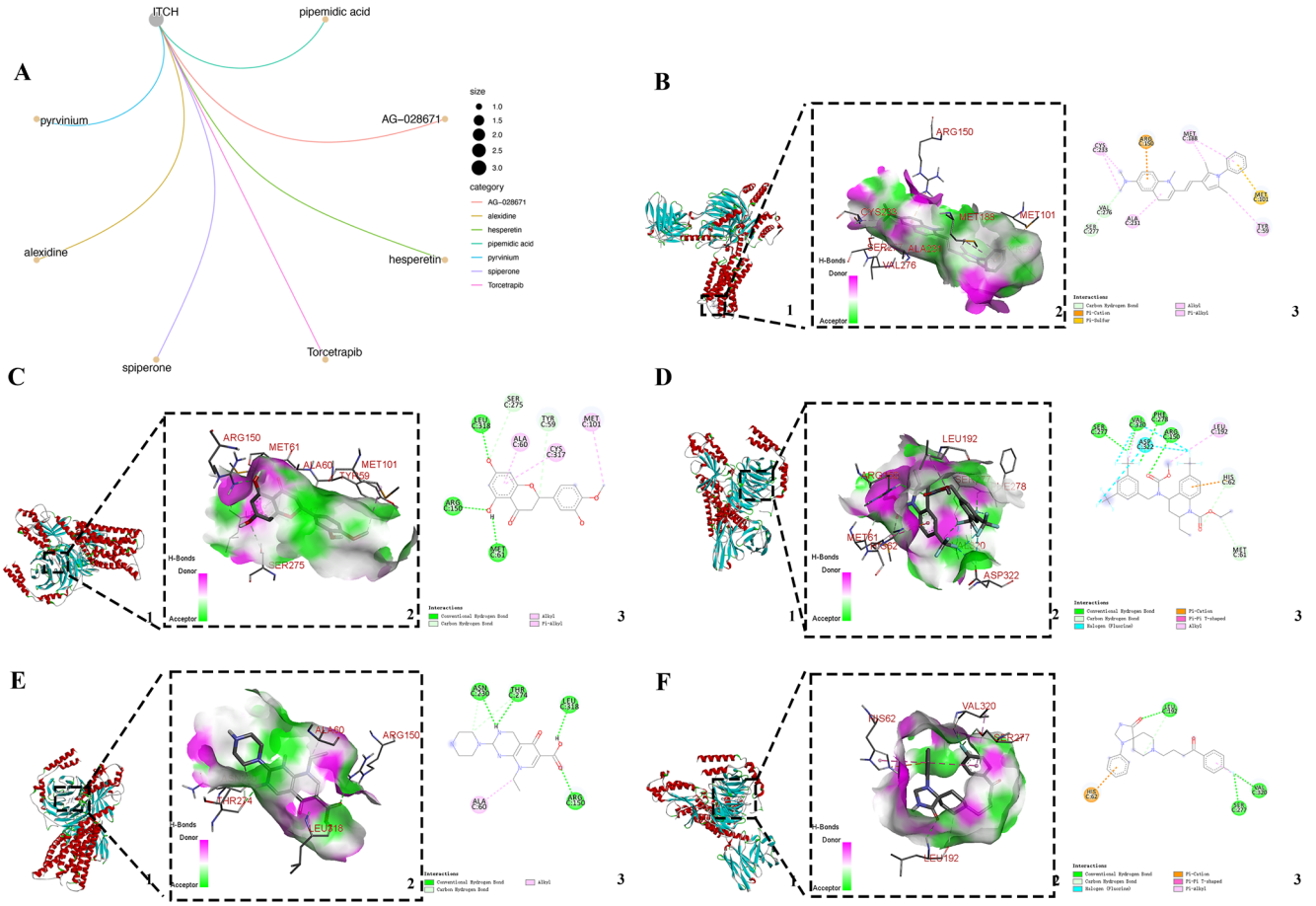

FIGURE 3 | The results of drug enrichment and molecular docking. (A) DSigDB-derived drug–gene network for ITCH; node size indicates significance and color denotes compound category. (B–F) Docking models of ITCH with pyrvinium (−8.8 kcal/mol), hesperetin (−8.0 kcal/mol), torcetrapib (−7.7 kcal/mol), pipemidic acid (−7.6 kcal/mol), and spiperone (−7.1 kcal/mol). For each complex: (1) overall binding pose, (2) pocket view, and (3) 2D interaction map.

domain. The WW motifs mediate intramolecular interactions that maintain ITCH in an autoinhibited conformation under basal conditions [21]. Upon activation, ITCH facilitates ubiquitin transfer from E2 conjugating enzymes to substrate proteins, marking them for lysosomal or proteasomal degradation—a process central to its regulatory functions.

ITCH orchestrates diverse cellular processes by polyubiquitinating over 50 substrates, including c-JUN, c-FLIP, LATS1, NOTCH1, and SMAD2 [22]. A hallmark of ITCH is its regulatory role in apoptosis. For instance, c-FLIPL (Cellular FLICE-like inhibitory protein long isoform), a caspase-8 inhibitor under NF-κB transcriptional control, suppresses caspase-8 activation within the TNFα-induced death signaling complex (Complex II). Activated by JNK1 phosphorylation, ITCH specifically recognizes the caspase-like (CASP) domain of c-FLIPL, catalyzing its ubiquitination and proteasomal degradation. This relieves caspase-8 inhibition, thereby amplifying TNF-α-mediated apoptosis [23]. Analogously, ITCH enhances TRAIL-induced apoptosis by destabilizing c-FLIPL [24]. Beyond caspase-dependent pathways, ITCH governs mitochondrial apoptosis through ubiquitination-mediated degradation of the cholesterol transport complex STARD1/VDAC2. Reduced mitochondrial cholesterol preserves membrane fluidity, facilitating BAX oligomerization, cytochrome c release, and activation of the intrinsic apoptotic cascade. Conversely, ITCH knockdown stabilizes STARD1, elevating mitochondrial cholesterol levels, impairing BAX activation, and blunting cytochrome c efflux. This confers resistance to apoptosis-inducing agents (e.g., TRAIL, cisplatin) by suppressing mitochondrial apoptosis [25].

The pro-apoptotic effect of ITCH is unequivocal, but ITCH has an inhibitory effect on NOTCH1 with latent anti-apoptotic possibilities. ITCH suppresses Notch1 signaling via two distinct mechanisms: (1) ubiquitinating the Notch1 intracellular domain (ICD) in cooperation with the adaptor protein Numb, targeting it for degradation [26, 27], and (2) degrading JAG1, a ligand critical for Notch1 activation [28] Notch1 activation upregulates anti-apoptotic Bcl-2 while downregulating pro-apoptotic Bax, lowering the Bax/Bcl-2 ratio to inhibit mitochondrial apoptosis. Additionally, Notch1 enhances survivin expression to directly suppress caspase activity [29] and stabilizes endoplasmic reticulum homeostasis, attenuating unfolded protein response (UPR)-driven apoptosis [30]. Paradoxically, Notch1 inhibition with DAPT reduces apoptosis in diabetic nephropathy under hyperglycemic conditions [31] while Numb protects renal proximal tubule cells by antagonizing Notch signaling [32] suggesting context-dependent pro-apoptotic roles for Notch1. In addition, ITCH suppresses pro-apoptotic signals by ubiquitinating p53

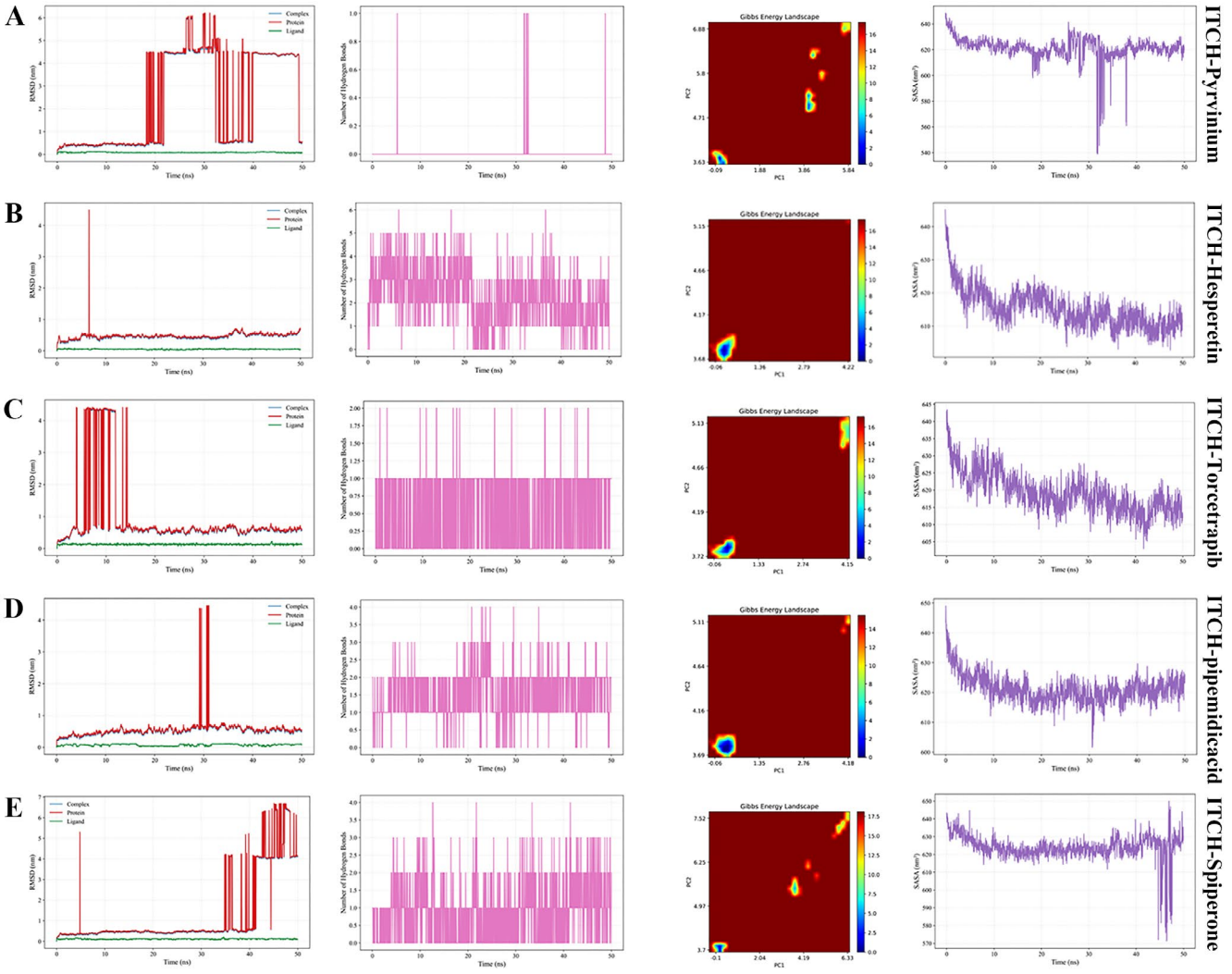

FIGURE 4 | MD-based stability profiling of ITCH–ligand complexes. (A–E) 50-ns MD trajectories for ITCH complexes with pyrvinium (A), hesperetin (B), torcetrapib (C), pipemidic acid (D), and spiperone (E). For each complex, panels show (from left to right): Backbone RMSD, protein–ligand hydrogen-bond counts, Gibbs free-energy landscape, and solvent-accessible surface area (SASA) over time.

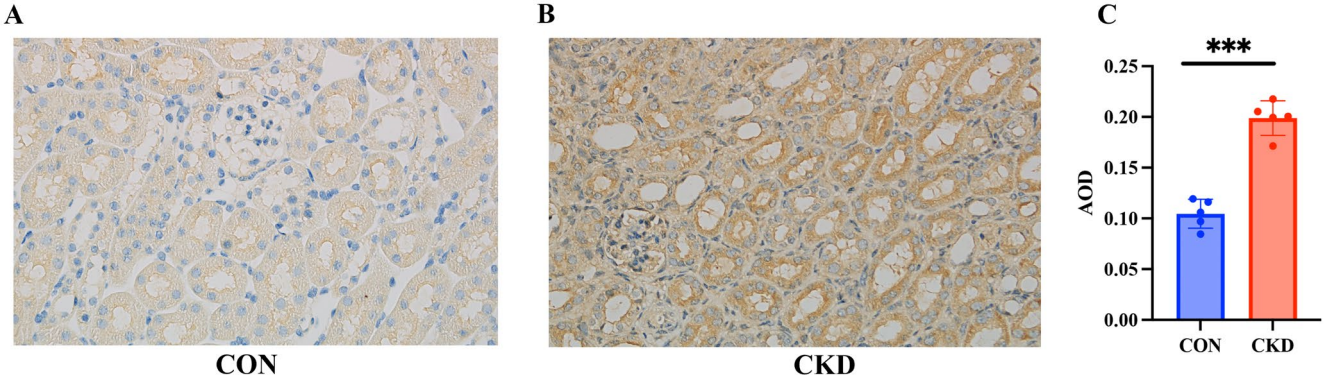

FIGURE 5 | Experimental validation of ITCH in CKD. (A, B) Representative images of ICTH immunohistochemical staining in kidney tissues from the control mouse and CKD. (400×) (C) Quantitative analysis of ITCH protein expression. The expression levels were determined by measuring the AOD within positively stained areas. Data are presented as the mean ± SEM of $n = 5$ mice per group. Statistical significance was assessed using an unpaired two-tailed Student's *t*-test (***$p < 0.001$ vs. control group).

family members (p73/p63) and the transcription factor c-Jun, promoting their proteasomal degradation [33]. This bidirectional regulation underscores ITCH's capacity to act as both a pro-survival and pro-apoptotic effector, contingent on cellular stress status.

Apoptosis, a programmed cell death mechanism, eliminates dysfunctional cells to maintain tissue homeostasis. Dysregulation—either excessive or insufficient—underlies diverse pathologies. In renal repair, apoptosis clears compensatory proliferating myofibroblasts and tubular cells post-injury [34, 35]. However, apoptosis has progressively become a pro-fibrotic accomplice in the development of CKD, a terminal CKD outcome marked by excessive ECM deposition. During AKI-CKD transition, maladaptive apoptosis accelerates nephron loss and fibrosis [36]. Key mediators include TGF-β-activated kinase 1 (TAK1), which induces apoptosis via p38 activation [37], and lncRNA Neat1, which sequesters miR-129-5p to exacerbate tubular apoptosis [38]. Consistently, clinical studies corroborate elevated apoptosis in CKD patients via ssDNA and TUNEL assays [39], while therapeutic attenuation of apoptosis improves renal function and fibrosis [40–43].

Apart from apoptosis, ITCH amplifies renal fibrosis by potentiating TGF-β signaling. ITCH enhances SMAD2 phosphorylation, fosters TGF-β receptor-SMAD2 complex formation [44], and degrades SMAD7 to amplify TGF-β responses [45]. Extracellular Matrix (ECM) stiffness further activates YAP1, driving TGF-β1 release and myofibroblast differentiation [46]. Parallel studies reveal ITCH destabilizes LATS1 via K48-linked polyubiquitination, relieving YAP/TAZ inhibition [47], suggesting a YAP/TAZ-mediated fibrogenic axis in CKD. ITCH also promotes fibrosis by facilitating cellular senescence, as previously shown in studies: Lysosomal-associated protein transmembrane 5 (LAPTM5) inhibited ubiquitination of Notch1 intracellular domain by mediating WWP2 lysosomal degradation and then leading to cellular senescence in tubular epithelial cells [48]. ITCH ubiquitinates Sirt6 [49], whose deficiency aggravates podocyte injury and proteinuria by dysregulating Notch1/Notch4 signaling [31]. Intriguingly, Notch1 doubly inhibits VE-cadherin expression through SNAI1 (snail family transcriptional repressor 1)-mediated transcriptional repression and loss of ERG (Ets related gene)-mediated transcriptional activation, thereby disrupting the paracellular and transcellular barrier functions of glomerular endothelial cells, ultimately leading to proteinuria [50].

ITCH exhibits its most significant expression in DCT, where its differential expression analysis is particularly valuable. However, to the best of our knowledge, a significant gap exists in the study of CKD specifically within the DCT, compared to research focused on proximal renal tubules and podocytes. Existing studies on the DCT have predominantly centered on its membrane sodium-chloride cotransporter (NCC) and its role in salt-sensitive hypertension associated with CKD [51], as well as mineral metabolism [52]. Notably, research indicates that Liver kinase B1 (LKB1) deficiency in the DCT contributes to CKD progression by inducing increased apoptosis [53].

Although this study possesses a degree of novelty and strengths, it nevertheless has its limitations. Firstly, despite employing aggregation strategies to circumvent pseudoreplication issues [54], the limited number of biological replicates constitutes a core limitation of this study, reducing its detection power. Secondly, cross-validation employing multiple MR methods was utilized to mitigate the impact of horizontal pleiotropy [55], though this inherent limitation cannot be eliminated. Further validation through experiments or other independent data sources remains necessary in future research. Thirdly, while molecular docking [56] and MD simulations provide preliminary evidence for the suitability of pharmacologically modulating ITCH, these remain computer-simulated outcomes whose biological efficacy requires rigorous in vitro and in vivo validation. Most critically, this study has thus far only confirmed ITCH expression alterations in CKD models via histochemical methods, representing a phenotypic association. The specific mechanisms governing whether and how ITCH functions as a core molecular driver of disease progression—including its upstream/downstream pathways and cell-specific actions—remain entirely unexplored "black boxes". Consequently, the therapeutic hypothesis proposed herein constitutes a framework derived from integrated bioinformatics analysis, awaiting comprehensive validation.

Taken as a whole, by integrating genetic and transcriptomic evidence, our findings not only expand our understanding of the molecular networks underlying CKD but also directly point toward novel translational medicine pathways for experimental interventions targeting ITCH.

Author Contributions

In this study, Xia Zhang and Dongdong Zhang jointly designed the research. Xia Zhang completed the article writing and molecular docking, while Dongdong Zhang handled data processing and bioinformatics analysis. Jiazhen Shang, Zhitao Zeng, Shouyu Chai, and Xincong Lv collaborated on the experimental validation portion. Zhimei Lv and Rong Wang supervised the project and provided resources, acting as co-corresponding authors.

Funding

This study was funded by the National Natural Science Foundation of China (Grant: 82370721, 82070744, 82300847) and Shandong Provincial Natural Science Foundation (No.: ZR2022LSW020, ZR2023LZY014, ZR2022QH151, ZR2024MH330).

Conflicts of Interest

The authors declare no conflicts of interest.

Data Availability Statement

If derived from public domain information.

References

1. A. C. Webster, E. V. Nagler, R. L. Morton, and P. Masson, "Chronic Kidney Disease," *Lancet* 389, no. 10075 (2017): 1238–1252, https://doi.org/10.1016/S0140-6736(16)32064-5.

2. K. J. Foreman, N. Marquez, A. Dolgert, et al., "Forecasting Life Expectancy, Years of Life Lost, and All-Cause and Cause-Specific Mortality for 250 Causes of Death: Reference and Alternative Scenarios for 2016–40 for 195 Countries and Territories," *Lancet* 392, no. 10159 (2018): 2052–2090, https://doi.org/10.1016/S0140-6736(18)31694-5.

3. P. Romagnani, R. Agarwal, J. C. N. Chan, et al., "Chronic Kidney Disease," *Nature Reviews. Disease Primers* 11, no. 1 (2025): 8, https://doi.org/10.1038/s41572-024-00589-9.

4. GBD Chronic Kidney Disease Collaboration, "Global, Regional, and National Burden of Chronic Kidney Disease, 1990–2017: A Systematic Analysis for the Global Burden of Disease Study 2017," *Lancet* 395, no. 10225 (2020): 709–733, https://doi.org/10.1016/S0140-6736(20)30045-3.

5. P. Romagnani, G. Remuzzi, R. Glassock, et al., "Chronic Kidney Disease," *Nature Reviews. Disease Primers* 3 (2017): 17088, https://doi.org/10.1038/nrdp.2017.88.

6. T. K. Chen, D. H. Knicely, and M. E. Grams, "Chronic Kidney Disease Diagnosis and Management: A Review," *Journal of the American Medical Association* 322, no. 13 (2019): 1294–1304, https://doi.org/10.1001/jama.2019.14745.

7. A. Khan and K. Kiryluk, "Kidney Disease Progression and Collider Bias in GWAS," *Kidney International* 102, no. 3 (2022): 476–478, https://doi.org/10.1016/j.kint.2022.06.018.

8. S. S. Potter, "Single-Cell RNA Sequencing for the Study of Development, Physiology and Disease," *Nature Reviews. Nephrology* 14, no. 8 (2018): 479–492, https://doi.org/10.1038/s41581-018-0021-7.

9. S. Park, S. Lee, Y. Kim, et al., "Atrial Fibrillation and Kidney Function: A Bidirectional Mendelian Randomization Study," *European Heart Journal* 42, no. 29 (2021): 2816–2823, https://doi.org/10.1093/eurheartj/ehab291.

10. C. A. de Leeuw, J. M. Mooij, T. Heskes, and D. Posthuma, "MAGMA: Generalized Gene-Set Analysis of GWAS Data," *PLoS Computational Biology* 11, no. 4 (2015): e1004219, https://doi.org/10.1371/journal.pcbi.1004219.

11. B. B. Lake, R. Menon, S. Winfree, et al., "An Atlas of Healthy and Injured Cell States and Niches in the Human Kidney," *Nature* 619, no. 7970 (2023): 585–594, https://doi.org/10.1038/s41586-023-05769-3.

12. J. B. Nielsen, R. B. Thorolfsdottir, L. G. Fritsche, et al., "Biobank-Driven Genomic Discovery Yields New Insight Into Atrial Fibrillation Biology," *Nature Genetics* 50, no. 9 (2018): 1234–1239, https://doi.org/10.1038/s41588-018-0171-3.

13. C. Pattaro, A. Teumer, M. Gorski, et al., "Genetic Associations at 53 Loci Highlight Cell Types and Biological Pathways Relevant for Kidney Function," *Nature Communications* 7 (2016): 10023, https://doi.org/10.1038/ncomms10023.

14. V. Zuber, N. F. Grinberg, D. Gill, et al., "Combining Evidence From Mendelian Randomization and Colocalization: Review and Comparison of Approaches," *American Journal of Human Genetics* 109, no. 5 (2022): 767–782, https://doi.org/10.1016/j.ajhg.2022.04.001.

15. C. Giambartolomei, D. Vukcevic, E. E. Schadt, et al., "Bayesian Test for Colocalisation Between Pairs of Genetic Association Studies Using Summary Statistics," *PLoS Genetics* 10, no. 5 (2014): e1004383, https://doi.org/10.1371/journal.pgen.1004383.

16. M. Yan, W. Li, R. Wei, et al., "Identification of Pyroptosis-Related Genes and Potential Drugs in Diabetic Nephropathy," *Journal of Translational Medicine* 21, no. 1 (2023): 490, https://doi.org/10.1186/s12967-023-04350-w.

17. Y. Liu, X. Yang, J. Gan, S. Chen, Z. X. Xiao, and Y. Cao, "CB-Dock2: Improved Protein-Ligand Blind Docking by Integrating Cavity Detection, Docking and Homologous Template Fitting," *Nucleic Acids Research* 50, no. W1 (2022): W159–W164, https://doi.org/10.1093/nar/gkac394.

18. X. Yang, Y. Liu, J. Gan, Z. X. Xiao, and Y. Cao, "FitDock: Protein-Ligand Docking by Template Fitting," *Briefings in Bioinformatics* 23, no. 3 (2022): bbac087, https://doi.org/10.1093/bib/bbac087.

19. A. R. Subramanya and D. H. Ellison, "Distal Convoluted Tubule," *Clinical Journal of the American Society of Nephrology* 9, no. 12 (2014): 2147–2163, https://doi.org/10.2215/CJN.05920613.

20. D. Rotin and S. Kumar, "Physiological Functions of the HECT Family of Ubiquitin Ligases," *Nature Reviews Molecular Cell Biology* 10, no. 6 (2009): 398–409, https://doi.org/10.1038/nrm2690.

21. M. D. Seo, S. J. Park, H. J. Kim, and B. J. Lee, "Identification of the WW Domain-Interaction Sites in the Unstructured N-Terminal Domain of EBV LMP 2A," *FEBS Letters* 581, no. 1 (2007): 65–70, https://doi.org/10.1016/j.febslet.2006.11.078.

22. Q. Yin, C. J. Wyatt, T. Han, K. S. M. Smalley, and L. Wan, "ITCH as a Potential Therapeutic Target in Human Cancers," *Seminars in Cancer Biology* 67, no. Pt 2 (2020): 117–130, https://doi.org/10.1016/j.semcancer.2020.03.003.

23. L. Chang, H. Kamata, G. Solinas, et al., "The E3 Ubiquitin Ligase Itch Couples JNK Activation to TNFalpha-Induced Cell Death by Inducing c-FLIP(L) Turnover," *Cell* 124, no. 3 (2006): 601–613, https://doi.org/10.1016/j.cell.2006.01.021.

24. F. Yang, K. H. Tay, L. Dong, et al., "Cystatin B Inhibition of TRAIL-Induced Apoptosis Is Associated With the Protection of FLIP(L) From Degradation by the E3 Ligase Itch in Human Melanoma Cells," *Cell Death and Differentiation* 17, no. 8 (2010): 1354–1367, https://doi.org/10.1038/cdd.2010.29.

25. J. Holloway, A. Seeley, N. Cobbe, R. C. Turkington, D. B. Longley, and E. Evergren, "The E3 Ubiquitin Ligase Itch Regulates Death Receptor and Cholesterol Trafficking to Affect TRAIL-Mediated Apoptosis," *Cell Death & Disease* 15, no. 1 (2024): 40, https://doi.org/10.1038/s41419-023-06417-4.

26. M. A. McGill and C. J. McGlade, "Mammalian Numb Proteins Promote Notch1 Receptor Ubiquitination and Degradation of the Notch1 Intracellular Domain," *Journal of Biological Chemistry* 278, no. 25 (2003): 23196–23203, https://doi.org/10.1074/jbc.M302827200.

27. W. Zhao, Y. Li, H. Cheng, et al., "Myofibrillogenesis Regulator-1 Regulates the Ubiquitin Lysosomal Pathway of Notch3 Intracellular Domain Through E3 Ubiquitin-Protein Ligase Itchy Homolog in the Metastasis of Non-Small Cell Lung Cancer," *Advanced Science* 11, no. 15 (2024): e2306472, https://doi.org/10.1002/advs.202306472.

28. L. Qi, M. Wang, J. He, B. Jia, J. Ren, and S. Zheng, "E3 Ubiquitin Ligase ITCH Improves LPS-Induced Chondrocyte Injury by Mediating JAG1 Ubiquitination in Osteoarthritis," *Chemico-Biological Interactions* 360 (2022): 109921, https://doi.org/10.1016/j.cbi.2022.109921.

29. S. Dabral, X. Tian, B. Kojonazarov, et al., "Notch1 Signalling Regulates Endothelial Proliferation and Apoptosis in Pulmonary Arterial Hypertension," *European Respiratory Journal* 48, no. 4 (2016): 1137–1149, https://doi.org/10.1183/13993003.00773-2015.

30. Q. Xie, Z. He, L. Tan, et al., "Hesperetin Induces Apoptosis in Lung Squamous Carcinoma Cells via G2/M Cycle Arrest, Inhibition of the Notch1 Pathway and Activation of Endoplasmic Reticulum Stress," *International Journal of Molecular Medicine* 55, no. 5 (2025): 77, https://doi.org/10.3892/ijmm.2025.5518.

31. M. Liu, K. Liang, J. Zhen, et al., "Sirt6 Deficiency Exacerbates Podocyte Injury and Proteinuria Through Targeting Notch Signaling," *Nature Communications* 8, no. 1 (2017): 413, https://doi.org/10.1038/s41467-017-00498-4.

32. X. Ding, F. Zhu, T. Li, Q. Zhou, F. F. Hou, and J. Nie, "Numb Protects Renal Proximal Tubular Cells From Puromycin Aminonucleoside-Induced Apoptosis Through Inhibiting Notch Signaling Pathway," *International Journal of Biological Sciences* 7, no. 3 (2011): 269–278, https://doi.org/10.7150/ijbs.7.269.

33. F. Bernassola, M. Karin, A. Ciechanover, and G. Melino, "The HECT Family of E3 Ubiquitin Ligases: Multiple Players in Cancer Development," *Cancer Cell* 14, no. 1 (2008): 10–21, https://doi.org/10.1016/j.ccr.2008.06.001.

34. Y. H. Chou, S. Y. Pan, Y. H. Shao, et al., "Methylation in Pericytes After Acute Injury Promotes Chronic Kidney Disease," *Journal of Clinical Investigation* 130, no. 9 (2020): 4845–4857, https://doi.org/10.1172/JCI135773.

35. A. Shimizu and N. Yamanaka, "Apoptosis and Cell Desquamation in Repair Process of Ischemic Tubular Necrosis," *Virchows Archiv. B, Cell Pathology Including Molecular Pathology* 64, no. 3 (1993): 171–180, https://doi.org/10.1007/BF02915110.

36. Z. Xia, Z. Wei, X. Li, et al., "C/EBPα Aggravates Renal Fibrosis in CKD Through the NOX4-ROS-Apoptosis Pathway in Tubular Epithelial Cells," *Biochimica et Biophysica Acta-Molecular Basis of Disease* 1870, no. 3 (2024): 167039, https://doi.org/10.1016/j.bbadis.2024.167039.

37. J. Zhou, J. Zhong, Z. Huang, et al., "TAK1 Mediates Apoptosis via p38 Involve in Ischemia-Induced Renal Fibrosis," *Artificial Cells, Nanomedicine, and Biotechnology* 46, no. sup1 (2018): 1016–1025, https://doi.org/10.1080/21691401.2018.1442841.

38. T. Ma, H. Li, H. Liu, et al., "Neat1 Promotes Acute Kidney Injury to Chronic Kidney Disease by Facilitating Tubular Epithelial Cells Apoptosis via Sequestering miR-129-5p," *Molecular Therapy* 30, no. 10 (2022): 3313–3332, https://doi.org/10.1016/j.ymthe.2022.05.019.

39. D. Verzola, V. Procopio, A. Sofia, et al., "Apoptosis and Myostatin mRNA Are Upregulated in the Skeletal Muscle of Patients With Chronic Kidney Disease," *Kidney International* 79, no. 7 (2011): 773–782, https://doi.org/10.1038/ki.2010.494.

40. F. C. Chang, C. H. Liu, A. J. Luo, et al., "Angiopoietin-2 Inhibition Attenuates Kidney Fibrosis by Hindering Chemokine C-C Motif Ligand 2 Expression and Apoptosis of Endothelial Cells," *Kidney International* 102, no. 4 (2022): 780–797, https://doi.org/10.1016/j.kint.2022.06.026.

41. N. Mehta, A. L. Gava, D. Zhang, B. Gao, and J. C. Krepinsky, "Follistatin Protects Against Glomerular Mesangial Cell Apoptosis and Oxidative Stress to Ameliorate Chronic Kidney Disease," *Antioxidants & Redox Signaling* 31, no. 8 (2019): 551–571, https://doi.org/10.1089/ars.2018.7684.

42. Y. Fan, J. Cheng, Q. Yang, et al., "Sirt6-Mediated Nrf2/HO-1 Activation Alleviates Angiotensin II-Induced DNA DSBs and Apoptosis in Podocytes," *Food & Function* 12, no. 17 (2021): 7867–7882, https://doi.org/10.1039/d0fo03467c.

43. G. Stokman, L. Kors, P. J. Bakker, et al., "NLRX1 Dampens Oxidative Stress and Apoptosis in Tissue Injury via Control of Mitochondrial Activity," *Journal of Experimental Medicine* 214, no. 8 (2017): 2405–2420, https://doi.org/10.1084/jem.20161031.

44. Y. Bai, C. Yang, K. Hu, C. Elly, and Y. C. Liu, "Itch E3 Ligase-Mediated Regulation of TGF-Beta Signaling by Modulating smad2 Phosphorylation," *Molecular Cell* 15, no. 5 (2004): 825–831, https://doi.org/10.1016/j.molcel.2004.07.021.

45. F. Lallemand, S. R. Seo, N. Ferrand, et al., "AIP4 Restricts Transforming Growth Factor-Beta Signaling Through a Ubiquitination-Independent Mechanism," *Journal of Biological Chemistry* 280, no. 30 (2005): 27645–27653, https://doi.org/10.1074/jbc.M500188200.

46. L. Li, H. Fu, and Y. Liu, "The Fibrogenic Niche in Kidney Fibrosis: Components and Mechanisms," *Nature Reviews. Nephrology* 18, no. 9 (2022): 545–557, https://doi.org/10.1038/s41581-022-00590-z.

47. Z. Salah, G. Melino, and R. I. Aqeilan, "Negative Regulation of the Hippo Pathway by E3 Ubiquitin Ligase ITCH Is Sufficient to Promote Tumorigenicity," *Cancer Research* 71, no. 5 (2011): 2010–2020, https://doi.org/10.1158/0008-5472.CAN-10-3516.

48. X. Liu, P. Zhan, Y. Zhang, et al., "Lysosomal-Associated Protein Transmembrane 5, Tubular Senescence, and Progression of CKD," *Journal of the American Society of Nephrology* 35, no. 12 (2024): 1655–1670, https://doi.org/10.1681/ASN.0000000000000446.

49. R. Stöhr, M. Mavilio, A. Marino, et al., "ITCH Modulates SIRT6 and SREBP2 to Influence Lipid Metabolism and Atherosclerosis in ApoE Null Mice," *Scientific Reports* 5, no. 1 (2015): 9023, https://doi.org/10.1038/srep09023.

50. L. Li, Q. Liu, T. Shang, et al., "Aberrant Activation of Notch1 Signaling in Glomerular Endothelium Induces Albuminuria," *Circulation Research* 128, no. 5 (2021): 602–618, https://doi.org/10.1161/CIRCRESAHA.120.316970.

51. T. Furusho, E. Sohara, S. Mandai, et al., "Renal TNFα Activates the WNK Phosphorylation Cascade and Contributes to Salt-Sensitive Hypertension in Chronic Kidney Disease," *Kidney International* 97, no. 4 (2020): 713–727, https://doi.org/10.1016/j.kint.2019.11.021.

52. H. Olauson, K. Lindberg, R. Amin, et al., "Targeted Deletion of Klotho in Kidney Distal Tubule Disrupts Mineral Metabolism," *Journal of the American Society of Nephrology* 23, no. 10 (2012): 1641–1651, https://doi.org/10.1681/ASN.2012010048.

53. S. H. Han, L. Malaga-Dieguez, F. Chinga, et al., "Deletion of Lkb1 in Renal Tubular Epithelial Cells Leads to CKD by Altering Metabolism," *Journal of the American Society of Nephrology* 27, no. 2 (2016): 439–453, https://doi.org/10.1681/ASN.2014121181.

54. K. D. Zimmerman, M. A. Espeland, and C. D. Langefeld, "A Practical Solution to Pseudoreplication Bias in Single-Cell Studies," *Nature Communications* 12, no. 1 (2021): 738, https://doi.org/10.1038/s41467-021-21038-1.

55. M. Verbanck, C. Y. Chen, B. Neale, and R. Do, "Detection of Widespread Horizontal Pleiotropy in Causal Relationships Inferred From Mendelian Randomization Between Complex Traits and Diseases," *Nature Genetics* 50, no. 5 (2018): 693–698, https://doi.org/10.1038/s41588-018-0099-7.

56. D. Ramírez and J. Caballero, "Is It Reliable to Use Common Molecular Docking Methods for Comparing the Binding Affinities of Enantiomer Pairs for Their Protein Target?," *International Journal of Molecular Sciences* 17, no. 4 (2016): 525, https://doi.org/10.3390/ijms17040525.

Supporting Information

Additional supporting information can be found online in the Supporting Information section. **Table S1:** Results of differential analysis. **Table S2:** Results of MR.